Combined solitary wave solutions for the inhomogeneous higher-order nonlinear Schrödinger equation

Rongcao Yang,* Lu Li, Ruiyu Hao, Zhonghao Li, and Guosheng Zhou†
College of Physics & Electronics Engineering and the State Key Subject of Optics, Shanxi University, Taiyuan, 030006, China
(Received 31 May 2004; revised manuscript received 12 August 2004; published 21 March 2005)

We consider the inhomogeneous higher-order nonlinear Schrödinger equation and explicitly present exact combined solitary wave solutions that can describe the simultaneous propagation of bright and dark solitary waves in a combined form in inhomogeneous fiber media or in optical communication links with distributed parameters. Furthermore, we analyze the features of the solutions, and numerically discuss the stabilities of these solitary waves under slight violations of the parameter conditions and finite initial perturbations. The results show that there exist combined solitary wave solutions in an inhomogeneous fiber system, and the combined solitary wave solutions are stable under slight violations of the parameter conditions and finite initial perturbations. Finally, the interaction between two neighboring combined solitary waves is numerically discussed.

DOI: 10.1103/PhysRevE.71.036616 PACS number(s): 42.81.Dp, 42.65.Tg, 05.45.Yv

It is well known that the propagation of subpicosecond or femtosecond optical pulse in fibers is described by the higher-order nonlinear Schrödinger (HNLS) equation including not only the group velocity dispersion (GVD) and self-phase-modulation (SPM), but also various higher-order effects, such as third-order dispersion (TOD), self-steepening, and self-frequency shift [1–3]. It has been extensively studied by many authors and some types of exact solitons or solitary wave solutions have been obtained [4–14]. It is worth noting that these investigations of optical solitons or solitary waves have been focused mainly on homogeneous fibers. However, in realistic fiber transmission lines, no fiber is homogeneous due to long distance communication and manufacturing problems. Recently, studies of the propagation of optical pulses in inhomogeneous fibers, which is described by the inhomogeneous nonlinear Schrödinger (INLS) type of equation, have attracted more interest. Many authors have investigated the INLS equations from different points of view (e.g., artificially induced inhomogeneity, randomly induced imperfections, soliton control and management, etc.) and obtained some exact soliton solutions for special parameter relations [15–28]. However, it should be noted that all of these studies are based on the INLS equation, in which the above-mentioned higher-order effects are omitted. Taking account of the higher-order effects influenced by the spatial variations of the fiber parameters, Papaioannou *et al.* first investigated the inhomogeneous higher-order nonlinear Schrödinger (IHNLS) equation, which describes femtosecond optical pulse propagation in inhomogeneous fibers, and derived exact bright and dark solitary wave solutions near the zero dispersion point [29]. To our knowledge, the study of the IHNLS equation has not been widespread.

In this paper, we consider the IHNLS equation and explicitly present three types of combined solitary wave solutions that describe the properties of both bright and dark solitary waves in the same expression. Furthermore, we analyze the features of the solutions, and numerically discuss the stabilities of these solitary waves under slight violations of the parameter conditions and finite initial perturbations. These results are useful in design of fiber optic amplifiers and in study of simultaneous propagation of bright and dark soliton-like pulses in femtosecond fiber laser systems or in optical communication links with distributed dispersion and nonlinearity management.

The governing envelope wave equation for femtosecond optical pulse propagation in inhomogeneous fiber takes the form [29]

$$q_z = i\alpha_1(z)q_{tt} + i\alpha_2(z)|q|^2q + \alpha_3(z)q_{ttt} + \alpha_4(z)(|q|^2q)_t + \alpha_5(z)q(|q|^2)_t + \Gamma(z)q, \tag{1}$$

where $q(z,t)$ represents the complex envelope of the electrical field, z is the normalized propagation distance, t is the normalized retarded time, and $\alpha_1(z)$, $\alpha_2(z)$, $\alpha_3(z)$, $\alpha_4(z)$, and $\alpha_5(z)$ are the distributed parameters, which are functions of the propagation distance z, related to GVD, SPM, TOD, self-steepening, and the delayed nonlinear response effect, respectively. $\Gamma(z)$ denotes the amplification or absorption coefficient. Study of Eq. (1) is of great interest due to its wide range of applications. Its use is not only restricted to optical pulse propagation in inhomogeneous fiber media, but also to the core of dispersion-managed solitons and combined-managed solitons.

First, we should point out that Eq. (1) is integrable for some special parameter conditions. For example, under the Hirota condition

$$3\alpha_3\alpha_2 = \alpha_4\alpha_1; \quad \alpha_4 + \alpha_5 = 0, \tag{2}$$

and the compatibility requirement

*Email address: sxdxyrc@sxu.edu.cn
†Email address: zhougs@sxu.edu.cn

$$\Gamma(z)=\frac{\alpha_{1,z}\alpha_2-\alpha_1\alpha_{2,z}}{2\alpha_1\alpha_2}, \tag{3}$$

one can follow the Ablowitz *et al.* formalism to construct the linear eigenvalue problem for bright and dark solitons of Eq. (1) as follows:

$$\Psi_t=U\Psi, \quad \Psi_z=V\Psi, \tag{4}$$

where $\Psi=(\Psi_1\ \Psi_2)^T$; here U and V can be given in the forms

$$U=\lambda J+P, \quad J=\begin{pmatrix}1 & 0\\ 0 & -1\end{pmatrix}, \quad P=\sqrt{\frac{\alpha_2}{2\mu\alpha_1}}\begin{pmatrix}0 & q\\ -\mu\overline{q} & 0\end{pmatrix}, \tag{5a}$$

$$V=\begin{pmatrix}A & B\\ C & -A\end{pmatrix}, \tag{5b}$$

with

$$A=4\alpha_3\lambda^3+2i\alpha_1\lambda^2+\frac{\alpha_2\alpha_3}{\alpha_1}|q|^2\lambda+\frac{\alpha_2\alpha_3}{2\alpha_1}(\overline{q}q_t-q\overline{q_t})+i\frac{\alpha_2}{2}|q|^2,$$

$$B=\sqrt{\frac{\alpha_2}{2\mu\alpha_1}}\left[4\alpha_3q\lambda^2+2(\alpha_3q_t+i\alpha_1q)\lambda+\alpha_3\left(q_{tt}+\frac{\alpha_2}{\alpha_1}q|q|^2\right)+i\alpha_1q_t\right],$$

$$C=\sqrt{\frac{\alpha_2}{2\mu\alpha_1}}\left[-4\mu\alpha_3\overline{q}\lambda^2+2\mu(\alpha_3\overline{q_t}-i\alpha_1\overline{q})\lambda-\mu\alpha_3\left(\overline{q_{tt}}+\frac{\alpha_2}{\alpha_1}\overline{q}|q|^2\right)+i\mu\alpha_1\overline{q_t}\right].$$

Here the overbar represents the complex conjugate, λ is a complex spectral parameter, and $\mu=\pm1$. It is easy to verify that, when $\mu=1$ and $\alpha_1\alpha_2>0$, the compatibility condition $U_z-V_t+[U,V]=0$ gives the IHNLS Eq. (1) for bright solitons; while when $\mu=-1$ and $\alpha_1\alpha_2<0$, the compatibility condition $U_z-V_t+[U,V]=0$ gives the IHNLS Eq. (1) for dark solitons. In general, the Lax pair (4) confirms that Eq. (1) is completely integrable under the above conditions (2) and (3), and is especially used to obtain the N-soliton solution (bright or dark soliton solution) by means of the inverse-scattering transform method. We could not yet obtain the Lax pair of Eq. (1) for combined solitary waves in spite of making great efforts to search for it. However, Eq. (1) is solvable for combined solitary waves under three sets of special parameter conditions as we show below.

Now we proceed with the analysis of Eq. (1) by separating $q(z,t)$ into the complex envelope function $A(z,t)$ and the phase shift $\varphi(z,t)=k(z)t+\Omega(z)$ according to $q(z,t)=A(z,t)\exp[i\varphi(z,t)]$. Substituting the expression into Eq. (1) and removing the exponential term, we can rewrite Eq. (1) as

$$iA_z+ia_1A_t+a_2A_{tt}-i\alpha_3A_{ttt}+a_4|A|^2A-ia_5|A|^2A_t-ia_6A^2A_t^*-(a_7+\varphi_z)A+i\Gamma A=0, \tag{6}$$

where $a_1=2\alpha_1k+3\alpha_3k^2$, $a_2=\alpha_1+3\alpha_3k$, $a_4=\alpha_2+\alpha_4k$, $a_5=2\alpha_4+\alpha_5$, $a_6=\alpha_4+\alpha_5$, and $a_7=\alpha_1k^2+\alpha_3k^3$, which are functions of the normalized distance z.

We introduce an ansatz similar to that of Refs. [12,13]

$$A(z,t)=i\beta(z)+\lambda(z)\tanh\{\eta(z)[t-\chi(z)]\}+i\rho(z)\mathrm{sech}\{\eta(z)[t-\chi(z)]\}, \tag{7}$$

where $\eta(z)$ and $\chi(z)$ are the pulse width and the shift of the inverse group velocity, respectively. Substituting the ansatz (7) into Eq. (6) and equating the coefficients of independent terms, one obtains

$$\eta_z=0, \tag{8a}$$

$$k_z=0, \tag{8b}$$

$$\beta_z+\Gamma\beta=0, \tag{8c}$$

$$\lambda_z+\Gamma\lambda=0, \tag{8d}$$

$$\rho_z+\Gamma\rho=0, \tag{8e}$$

$$\rho[2a_2\eta^2-a_4(\rho^2-\lambda^2)+2a_5\beta\lambda\eta]=0, \tag{8f}$$

$$\lambda[2a_2\eta^2-a_4(\rho^2-\lambda^2)]+2\beta\eta[a_5\rho^2+a_6(\rho^2-\lambda^2)]=0, \tag{8g}$$

$$\rho\eta[6\alpha_3\eta^2-(a_5+a_6)(\rho^2-\lambda^2)]=0, \tag{8h}$$

$$\lambda\eta[6\alpha_3\eta^2-(a_5+a_6)(\rho^2-\lambda^2)]=0, \tag{8i}$$

$$a_4\beta(3\rho^2-\lambda^2)+\lambda\eta[8\alpha_3\eta^2+a_1-a_5(\beta^2+2\rho^2-\lambda^2)+a_6(\beta^2+\lambda^2)-\chi_z]=0, \tag{8j}$$

$$2a_4\beta\lambda\rho+\rho\eta[5\alpha_3\eta^2+a_1-a_5(\beta^2+\rho^2)-a_6(\beta^2+\rho^2-2\lambda^2)-\chi_z]=0, \tag{8k}$$

$$\lambda[2a_2\eta^2-a_4(\beta^2+\rho^2)+a_7+\Omega_z]+2\beta\eta[a_5\rho^2+a_6(\rho^2-\lambda^2)]=0, \tag{8l}$$

$$\rho[a_2\eta^2-a_4(3\beta^2+\rho^2)+a_7+\Omega_z]+2\beta\lambda\rho\eta(a_5-a_6)=0, \tag{8m}$$

$$\beta[a_4(\beta^2+3\rho^2)-a_7-\Omega_z]+\lambda\eta[2\alpha_3\eta^2+a_1-a_5(\beta^2+\rho^2)+a_6(\beta^2+\rho^2)-\chi_z]=0. \tag{8n}$$

From Eqs. (8a)–(8n), one can see that when the gain and/or loss distributed function $\Gamma=0$, the system parameters $\alpha_1,\alpha_2,\alpha_3,\alpha_4,\alpha_5$, and the solitary wave parameters $\eta,k,\beta,\lambda,\rho,\chi,\Omega$ are independent of z, these 14 equations can be reduced to nine equations, and the corresponding results agree with Ref. [12], in which three types of combined solitary wave solutions for the HNLS equation with constant coefficients have been discussed in detail. Also, in the special case of $\beta=\lambda=0$ or $\rho=0$, Eqs. (8a)–(8n) are reduced to seven or nine equations, and one can obtain the corresponding bright or dark solitary wave solution for the IHNLS equation, which has been obtained recently in Refs. [30,31]. Notice that, as $\alpha_3=\alpha_4=\alpha_5=0$, Eq. (1) can reduce to the INLS equation and then the 14 equations mentioned above are not compatible, which means that it is impossible that such a combined solitary wave solution (7) could exist for the INLS equation. The result is similar to that of the NLS equation with constant coefficients [12].

Now we continue the analysis of Eqs. (8a)–(8n). From Eqs. (8a)–(8e) one can obtain

$$\eta = \eta_c, \tag{9}$$

$$k = k_c, \tag{10}$$

$$\beta(z) = \beta_0 \exp\left[-\int_0^z \Gamma(\varsigma)d\varsigma\right], \tag{11}$$

$$\lambda(z) = \lambda_0 \exp\left[-\int_0^z \Gamma(\varsigma)d\varsigma\right], \tag{12}$$

$$\rho(z) = \rho_0 \exp\left[-\int_0^z \Gamma(\varsigma)d\varsigma\right], \tag{13}$$

where η_c and k_c are arbitrary constants, and β_0, λ_0, and ρ_0 are integral constants related to the initial pulse injection, respectively. From Eqs. (11)–(13), one can see clearly that the amplitude of the pulse is not a constant due to the presence of $\Gamma(z)$, and increases or decreases along the propagation direction of the fiber depending on the sign of $\Gamma(z)$. Equations (9) and (10) imply that the pulse width and the wave number remain constant during propagation along the fiber. For Eqs. (8f)–(8n), similarly to Ref. [12], there are the following three cases.

(i) $\alpha_1/3\alpha_3=\alpha_2/\alpha_4=\text{const}$, $\alpha_4+2\alpha_5=0$, and $\Gamma=(\alpha_1\alpha_{2,z}-\alpha_{1,z}\alpha_2)/2\alpha_1\alpha_2$. In this case, the solution (7) can be written as

$$A(z,t) = \lambda(z)\tanh\{\eta_c[t-\chi(z)]\} + i\rho(z)\operatorname{sech}\{\eta_c[t-\chi(z)]\}, \tag{14}$$

and its intensity is given by

$$|A|^2 = (\lambda_0^2 + (\rho_0^2-\lambda_0^2)\operatorname{sech}^2\{\eta_c[t-\chi(z)]\}) \times \exp\left[-2\int_0^z \Gamma(\varsigma)d\varsigma\right], \tag{15}$$

where

$$\eta_c^2 = \frac{\alpha_4(z)}{3\alpha_3(z)}(\rho_0^2-\lambda_0^2)\exp\left[-2\int_0^z \Gamma(\varsigma)d\varsigma\right], \tag{16}$$

$$k_c = -\frac{\alpha_2(z)}{\alpha_4(z)}, \tag{17}$$

$$\chi(z) = 2k_c\int_0^z \alpha_1(\varsigma)d\varsigma + (3k_c^2-\eta_c^2)\int_0^z \alpha_3(\varsigma)d\varsigma - \lambda_0^2\int_0^z \alpha_4(\varsigma)\exp\left[-2\int_0^\varsigma \Gamma(\xi)d\xi\right]d\varsigma, \tag{18}$$

$$\Omega(z) = -k_c^2\int_0^z \alpha_1(\varsigma)d\varsigma - k_c^3\int_0^z \alpha_3(\varsigma)d\varsigma. \tag{19}$$

From Eq. (16) one can see that system parameters $\alpha_3(z)$ and $\alpha_4(z)$, and the gain and/or loss distributed function $\Gamma(z)$ must satisfy

$$[\alpha_4(z)/\alpha_3(z)]\exp[-2\int_0^z \Gamma(\varsigma)d\varsigma] = \text{const}$$

except for $\alpha_3\alpha_4(\rho_0^2-\lambda_0^2)>0$, since η_c is a constant. In this situation, the solution (14) describes a brightlike or darklike solitary wave (depending on the sign of the factor $\rho_0^2-\lambda_0^2$) with a variable platform $\lambda_0\exp[-\int_0^z\Gamma(\varsigma)d\varsigma]$. We note that the time shift $\chi(z)$ and the group velocity $V(z)=d\chi/dz$ of the solitary wave are dependent on z, which leads to a change of the center position of the solitary wave along the propagation direction of the fiber, and means that we may design a fiber system to control the time shift and the velocity of the solitary wave. In order to understand the evolution of the solution (14), let us consider a soliton management system similar to that of Ref. [23], where the system parameters are of the forms

$$\alpha_1(z) = \alpha_{10}\exp(\sigma z)\cos(gz), \tag{20a}$$

$$\alpha_2(z) = \alpha_{20}\cos(gz), \tag{20b}$$

$$\alpha_3(z) = \alpha_{30}\exp(\sigma z)\cos(gz), \tag{20c}$$

$$\alpha_4(z) = \alpha_{40}\cos(gz), \tag{20d}$$

where α_{10}, α_{30}, and σ are parameters related to the GVD and TOD, and α_{20} and α_{40} denote the nonlinearity and self-steepening, respectively. g is related to the variation period of the fiber parameters. In this situation, the gain and/or loss distributed function $\Gamma(z)$ is of the constant form $\Gamma(z)=-\sigma/2$, which corresponds to a dispersion decreasing fiber for $\sigma<0$. Figure 1 presents the evolution plots of the solution (14) for different signs of $\rho_0^2-\lambda_0^2$ in this system with $\sigma<0$. From it one can clearly see that the intensity of the solitary wave decreases when $\sigma<0$, and the time shift and the group velocity of the solitary wave are changing while the solitary wave keeps its shape in propagating along the fiber. This is one of the important properties of solitary waves.

(ii) $\alpha_3=0$, $\alpha_4+\alpha_5=0$, $\alpha_2/\alpha_4=\text{const}$, and $\Gamma=(\alpha_1\alpha_{4,z}-\alpha_{1,z}\alpha_4)/2\alpha_1\alpha_4$. In this case, the solution (7) can be written in the form

$$A(z,t) = i\beta(z) + \lambda(z)\tanh\{\eta_c[t-\chi(z)]\} \pm i\lambda(z) \times\operatorname{sech}\{\eta_c[t-\chi(z)]\}, \tag{21}$$

and its intensity is given by

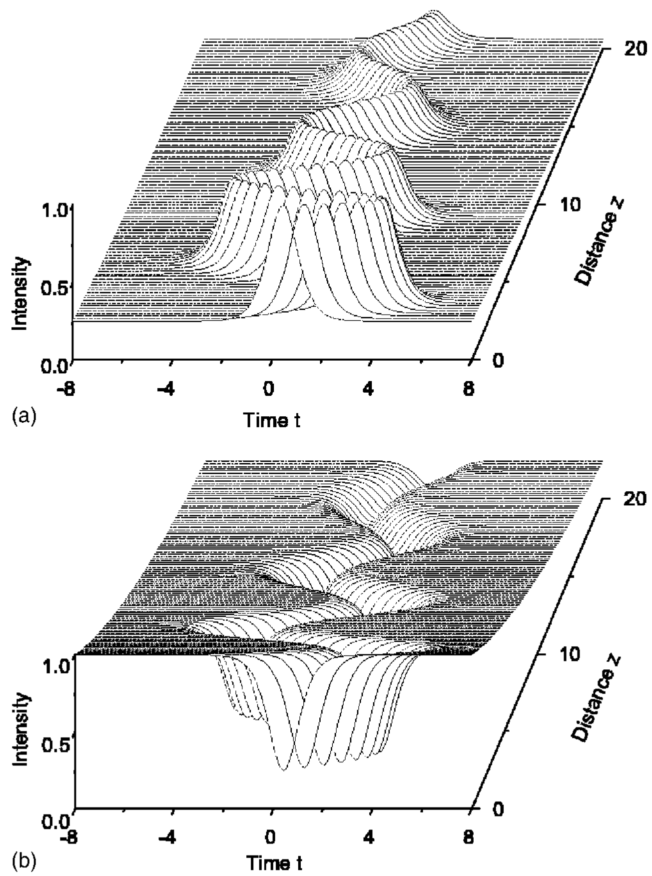

FIG. 1. The evolution plots of the combined solitary wave solution (14) for (a) a brightlike and (b) a darklike solitary wave in the system (20) with parameters as follows: $\sigma=-0.07$, $g=1$, $\alpha_{20}=1$, $\alpha_{30}=-0.02$; (a) $\alpha_{10}=0.5$, $\rho_0=1$, $\lambda_0=0.5$, and (b) $\alpha_{10}=-0.5$, $\lambda_0=1$, $\rho_0=0.5$.

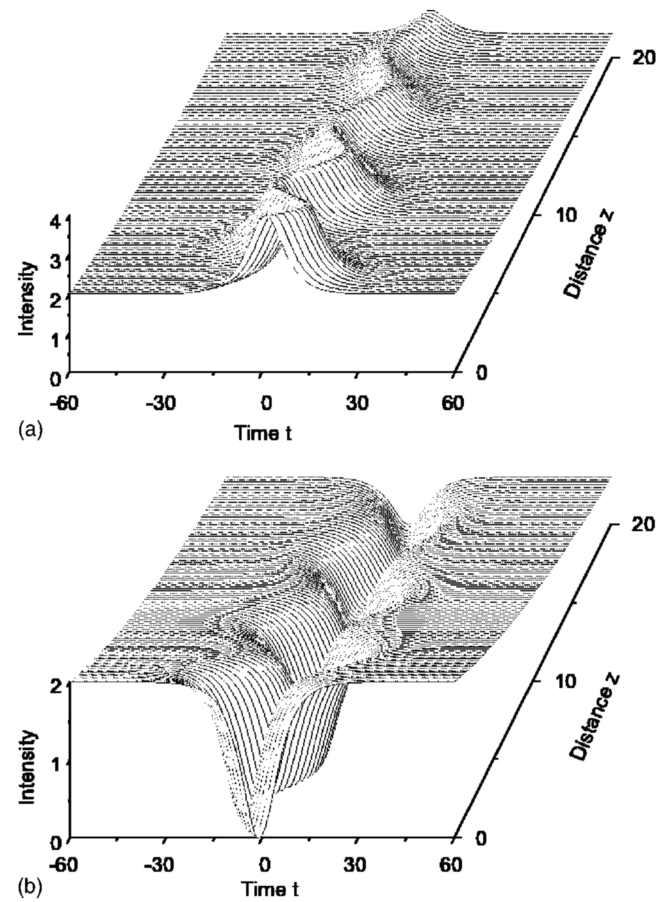

FIG. 2. The evolution plots of the combined solitary wave solution (21) for (a) a brightlike and (b) a darklike solitary wave in the system (20) with parameters as follows: $\sigma=-0.06$, $g=1$, $\alpha_{20}=1$, $\alpha_{30}=0$, $\alpha_{40}=-0.1$; (a) $\alpha_{10}=0.5$, $\lambda_0=1$, $\beta_0=1$ and (b) $\alpha_{10}=-0.5$, $\lambda_0=1$, $\beta_0=-1$.

$$|A|^2=(\beta_0^2+\lambda_0^2\pm 2\beta_0^2\lambda_0^2\mathrm{sech}\{\eta_c[t-\chi(z)]\})\times\exp\left[-2\int_0^z\Gamma(\varsigma)d\varsigma\right], \tag{22}$$

where

$$\eta_c=-\frac{\alpha_4(z)}{\alpha_1(z)}\lambda_0\beta_0\exp\left[-2\int_0^z\Gamma(\varsigma)d\varsigma\right], \tag{23}$$

$$k_c=-\frac{\alpha_2(z)}{\alpha_4(z)}-\frac{\alpha_4(z)}{2\alpha_1(z)}\lambda_0^2\exp\left[-2\int_0^z\Gamma(\varsigma)d\varsigma\right], \tag{24}$$

$$\chi(z)=-2\int_0^z\frac{\alpha_1(\varsigma)\alpha_2(\varsigma)}{\alpha_4(\varsigma)}d\varsigma-(\beta_0^2+\lambda_0^2)\int_0^z\alpha_4(\varsigma)\times\exp\left[-2\int_0^\varsigma\Gamma(\xi)d\xi\right]d\varsigma, \tag{25}$$

$$\Omega(z)=-k_c^2\int_0^z\alpha_1(\varsigma)d\varsigma+(\beta_0^2+\lambda_0^2)\int_0^z[\alpha_2(\varsigma)+k_c\alpha_4(\varsigma)]\times\exp\left[-2\int_0^\varsigma\Gamma(\xi)d\xi\right]d\varsigma. \tag{26}$$

Similarly to the case (i), we can see from Eqs. (23) and (24) that the parameters $\alpha_1(z),\alpha_4(z)$, and the gain and/or loss distributed function $\Gamma(z)$ must satisfy

$$[\alpha_4(z)/\alpha_1(z)]\exp[-2\int_0^z\Gamma(\varsigma)d\varsigma]=\mathrm{const},$$

since η_c and k_c are constants. In this case, the solution (21) presents a brightlike or darklike solitary wave depending on the sign of $\lambda_0\beta_0$. However, unlike the case (i), the solution (21) does not depend on special features of medium intensity and is dependent only on the initial pulse. This feature indicates that a bright and dark solitary wave may combine together under certain conditions and propagate simultaneously in an inhomogeneous fiber in a combined form. Figure 2 presents the evolution plots of the solution (21) for different signs of $\lambda_0\beta_0$ in the system (20).

(iii) $\alpha_1=\alpha_3=3\alpha_4+2\alpha_5=0$ and $W[\alpha_2,\alpha_4]=\alpha_{2,z}\alpha_4-\alpha_2\alpha_{4,z}$

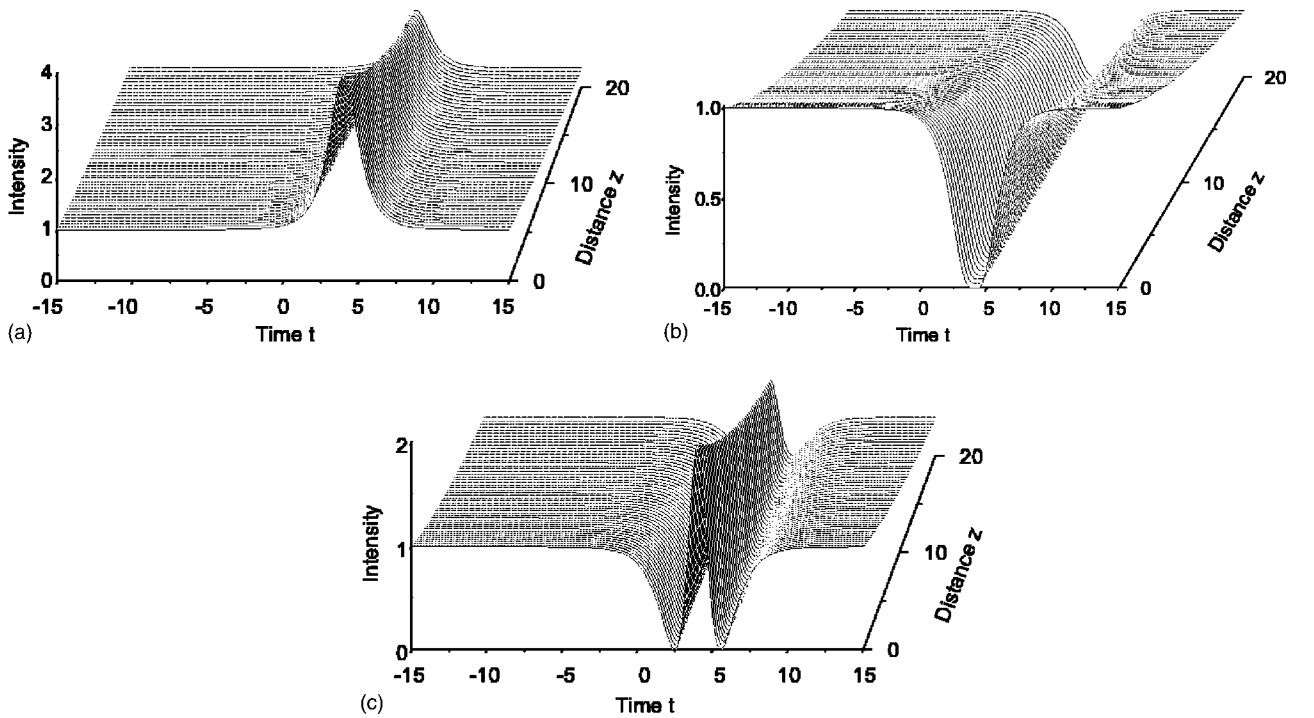

FIG. 3. The evolution plots of the combined solitary wave solution (33) for (a) a brightlike, (b) a darklike, and (c) a W-shape solitary wave in the system (20) with parameters as follows: $\sigma=-0.05$, $g=1$, $\alpha_{10}=0$, $\alpha_{20}=1$, $\alpha_{30}=0$, $\alpha_{40}=0.1$; (a) $\rho_0=1$, $\beta_0=1$, (b) $\rho_0=-1$, $\beta_0=1$, and (c) $\rho_0=-(1+\sqrt{2})$, $\beta_0=1$.

$=0$. In this case, the solution (7) can be written as

$$A(z,t) = i\beta(z) + \lambda(z)\tanh\{\eta_c[t-\chi(z)]\} + i\rho(z)\mathrm{sech}\{\eta_c[t-\chi(z)]\}, \tag{27}$$

and its intensity is given by

$$|A|^2 = (\beta_0^2 + \lambda_0^2 + 2\beta_0\rho_0\mathrm{sech}\{\eta_c[t-\chi(z)]\} + (\rho_0^2 - \lambda_0^2)\mathrm{sech}^2\{\eta_c[t-\chi(z)]\})\exp[-2\int_0^z \Gamma(\varsigma)d\varsigma], \tag{28}$$

where

$$\eta_c = -\frac{[\alpha_2(z) + k_c\alpha_4(z)]\beta_0}{[\alpha_4(z) + \alpha_5(z)]\lambda_0}, \tag{29}$$

$$\rho_0^2 = 2\beta_0^2 + \lambda_0^2, \tag{30}$$

$$\chi(z) = \mathrm{const}, \tag{31}$$

$$\Omega(z) = (\beta_0^2 + \lambda_0^2)\int_0^z [\alpha_2(\varsigma) + k_c\alpha_4(\varsigma)]\exp\left[-2\int_0^\varsigma \Gamma(\xi)d\xi\right]d\varsigma. \tag{32}$$

Similarly, Eq. (29) requires that $[\alpha_2(z)+k_c\alpha_4(z)]/[\alpha_4(z)+\alpha_5(z)]$ is a constant. The combined solitary wave (27) may be used in some dispersion compensation systems and laser systems, etc. Here we consider the special case of $\lambda=0$ and then the solution (27) can reduce the envelope function of the electrical field to the following form:

$$q(z,t) = \{i\beta(z) + i\rho(z)\mathrm{sech}[\eta_c(t-\chi_c)]\}\exp\left[-i\left(\frac{\alpha_2}{\alpha_4}t + \Omega_c\right)\right], \tag{33}$$

and its intensity is given by

$$|q|^2 = \{\beta_0^2 + \rho_0^2\mathrm{sech}^2[\eta_c(t-\chi_c)] + 2\beta_0\rho_0\,\mathrm{sech}[\eta_c(t-\chi_c)]\} \times\exp\left[-2\int_0^z \Gamma(\varsigma)d\varsigma\right], \tag{34}$$

where χ_c and Ω_c are arbitrary constants. The intensity of the solitary wave (33) takes different shapes under different pulse parameters. When $\beta_0\rho_0>0$, the solution (33) represents a brightlike solitary wave, and when $\beta_0\rho_0<0$ and $|\rho_0|\leqslant|\beta_0|$, the solution (33) represents a darklike solitary wave, as shown in Figs. 3(a) and 3(b), respectively. However, when $\beta_0\rho_0<0$ and $|\rho_0|>|\beta_0|$, the solution (33) represents a W-shaped solitary wave, as shown Fig. 3(c). It is worth noting that, unlike the previous two cases, the solitary velocity does not change and there is only a changeless time shift in propagation due to constant χ_c. In particular, when $\chi_c=\Omega_c=0$ and $\Gamma(z)=0$, the solution (33) is in agreement with the one of Ref. [12]. This means that this type of combined solitary wave has a more general form than the earlier report [12].

We have investigated the general character of the combined solitary wave solution from the soliton management concept by considering the system (20). In practical fiber

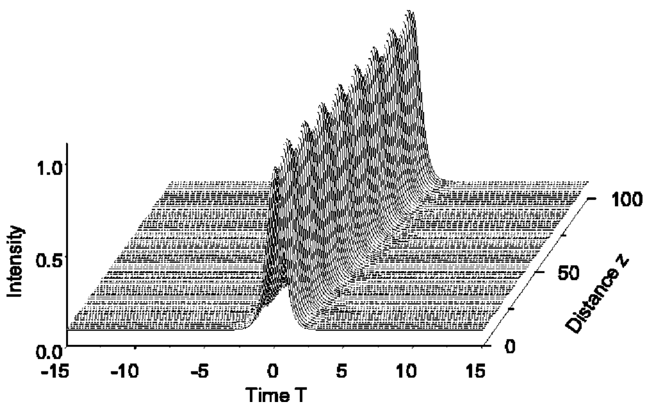

FIG. 4. The evolution plot of the combined solitary wave solution (14) under the strict constraint conditions (36) and (37) with parameters as follows: $\varepsilon_1=\varepsilon_3=0.05$, $\varepsilon_2=\varepsilon_4=0.1$, $g=0.5$, $\alpha_{10}=0.5$, $\alpha_{20}=1$, $\alpha_{30}=-0.01$, $\lambda_0=0.3$, $\rho_0=1$.

communication, however, it is difficult to produce an ideal homogeneous fiber system due to manufacturing imperfections. If the inhomogeneity is relatively small, one may assume that the fiber parameters simply fluctuate in a sinusoidal form around the values of the ideal fiber parameters. Therefore, in the following, we will consider a practical inhomogeneous fiber system, where the fiber parameters are of the forms

$$\alpha_1(z)=\alpha_{10}[1+\varepsilon_1\sin(gz)], \tag{35a}$$

$$\alpha_2(z)=\alpha_{20}[1+\varepsilon_2\sin(gz)], \tag{35b}$$

$$\alpha_3(z)=\alpha_{30}[1+\varepsilon_3\sin(gz)], \tag{35c}$$

$$\alpha_4(z)=\alpha_{40}[1+\varepsilon_4\sin(gz)], \tag{35d}$$

where α_{10}, α_{20}, α_{30}, and α_{40} are ideal fiber parameters, and ε_j, $j=1,2,3,4$, are small quantities that characterize the amplitudes of fluctuations. In order to understand the influence of such small fluctuations of the fiber parameters on the combined solitary wave, here we take the case (i) as an example to discuss the evolution of the combined solitary wave (7). In this situation, there exists an exact combined solitary wave solution (14) with $\lambda(z)=\lambda_0\sqrt{[1+\varepsilon_1\sin(gz)]/[1+\varepsilon_2\sin(gz)]}$ and $\rho(z)=\rho_0\sqrt{[1+\varepsilon_1\sin(gz)]/[1+\varepsilon_2\sin(gz)]}$ under the constraint conditions

$$3\alpha_{20}\alpha_{30}=\alpha_{10}\alpha_{40},\quad \varepsilon_1=\varepsilon_3,\quad \varepsilon_2=\varepsilon_4,\quad \alpha_4+2\alpha_5=0, \tag{36}$$

and

$$\Gamma(z)=\frac{g(\varepsilon_2-\varepsilon_1)\cos(gz)}{2[1+\varepsilon_1\sin(gz)][1+\varepsilon_2\sin(gz)]}. \tag{37}$$

Figure 4 shows the evolution plot of the combined solitary wave solution (14) under these strict constraint conditions. It should be pointed out that, for convenience, the transformation of the time coordinate $T=t-[2k_c\int_0^z\alpha_1(\varsigma)d\varsigma+(3k_c^2-\eta_c^2)\int_0^z\alpha_3(\varsigma)d\varsigma]$ is used in Fig. 4 as well as the following

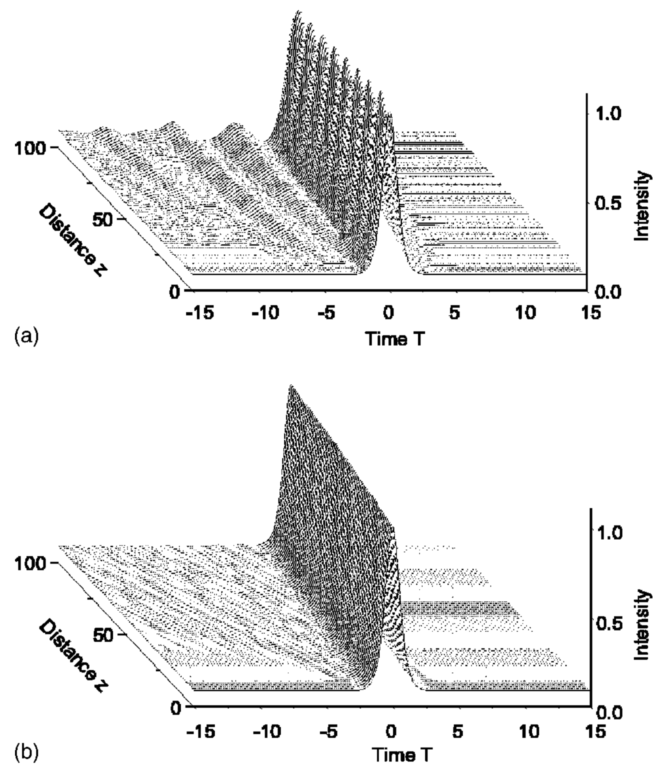

FIG. 5. The numerical evolution of the combined solitary wave (14) with $\lambda_0=0.3$, $\rho_0=1$ in the system (35) under slight violations of the parameter conditions: (a) $\alpha_{10}=0.485$, the other parameters the same as in Fig. 4; (b) $\varepsilon_1=0.05$, $\varepsilon_2=0.09$, $\varepsilon_3=0.0475$, $\varepsilon_4=0.1$, $\alpha_{40}=-0.06$, $\alpha_{50}=0.027$, $\Gamma(z)=0$, the other parameters the same as in Fig. 4.

figures. It can be seen from Fig. 4 that the intensity and platform of the solitary wave vary with propagation distance since $\Gamma(z)\neq$ const, while the pulse width stays constant as it propagates along the fiber. It should be noted that the above solitary wave solution is based on the corresponding constraint conditions (36) and (37) which present the balances among the ideal fiber parameters and the fluctuation parameters. In real applications, however, it may be difficult to produce such exact balances. Therefore, a study for the perturbed constraint conditions (36) and (37) is necessary. In Figs. 5(a) and 5(b), we present the numerical evolution of the combined solitary wave solution (14) under two different slight violations of the constraint conditions: (a) $3\alpha_{20}\alpha_{30}=0.97\alpha_{10}\alpha_{40}$ and the other conditions do not change; (b) $\varepsilon_1=0.95\varepsilon_3$, $0.9\times\varepsilon_2=\varepsilon_4$, $0.9\times\alpha_4+2\alpha_5=0$, $\Gamma(z)=0$, and the condition $3\alpha_{20}\alpha_{30}=\alpha_{10}\alpha_{40}$ does not change. From Fig. 5 we can see that the profiles of the solitary wave do not change except for some small oscillations on one side of the platform. Notice that the intensity and platform are not variable in Fig. 5(b) due to the perturbed condition $\Gamma(z)=0$. By comparing Fig. 5(a) with 5(b), we find that the condition $3\alpha_{20}\alpha_{30}=\alpha_{10}\alpha_{40}$ has a stronger influence on the solitary wave propagation than the others.

In order to analyze the stability of these solitary wave solutions with respect to finite initial perturbations, we still take the case (i) as an example to perform two types of numerical experiments for the system (35). First, we perturb

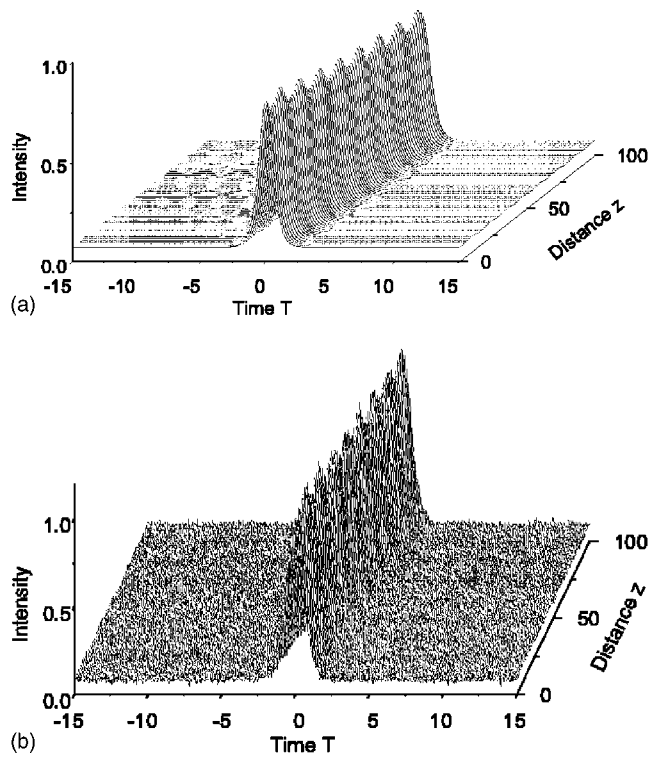

FIG. 6. The numerical evolution of (a) an initial pulse whose amplitude is 10% smaller than the theoretical prediction, i.e., 0.9; (b) the exact solution under the perturbation of white noise in the system (35) with the same parameters as in Fig. 4.

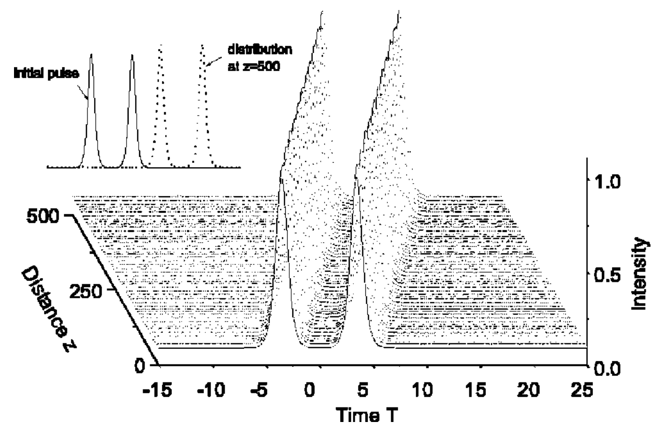

FIG. 7. The interaction scenario of two neighboring solitary waves (38) in the system (35) when the initial separation is equal to 7. The adopted parameters are the same as in Fig. 4.

the amplitude (10%) in the initial distribution. Second, we add white noise in an initial pulse $[\lambda_0 \tanh(\eta_c t) + i\rho_0 \operatorname{sech}(\eta_c t)]\exp(ik_c t) + 0.1\text{random}(t)$. The numerical results are shown in Figs. 6(a) and 6(b), respectively. The results reveal that the combined solitary wave can propagate in a stable way under finite initial perturbations, such as amplitude and white noise.

In addition, we consider the interaction between two neighboring solitary waves (14) in the system (35). The input pulse is of the form

$$q(0,t) = \{\lambda_0 \tanh[\eta_c(t + t_0/2)] + i\rho_0 \operatorname{sech}[\eta_c(t + t_0/2)]\} \times \exp(ik_c t) \tag{38a}$$

as $-\infty < t < 0$, and

$$q(0,t) = \{-\lambda_0 \tanh[\eta_c(t - t_0/2)] + i\rho_0 \operatorname{sech}[\eta_c(t - t_0/2)]\} \times \exp(ik_c t) \tag{38b}$$

as $0 \leqslant t < +\infty$. Here t_0 is the initial separation between two neighboring solitary waves. Figure 7 presents the interaction scenario of two neighboring solitary waves (38) with the initial separation $t_0 = 7$, where the parameters adopted are the same as in Fig. 4. From it one can clearly see that the two solitary waves hardly interact and the separation stays constant while propagating 500 dispersion lengths along the fiber. However, when the initial separation decreases further, the interaction between two neighboring solitary waves becomes serious and repulsion occurs. This particular property might come from the combination of bright and dark solitary waves. Also, by a lot of numerical simulations, we find that the separation of the neighboring combined solitary waves in Eq. (38) is smaller than that of the pure bright or dark solitons. Therefore, we may infer that the combined transmission of bright and dark solitary waves can restrict the interaction between the neighboring solitary waves to some extent. This is an advantage in improving the information bit rate in ultrahigh-speed optical telecommunication.

In conclusion, we have investigated the IHNLS equation and presented three types of combined solitary wave solutions in explicit forms for the wave propagation in an inhomogeneous fiber system using the complex amplitude ansatz method. The results show that there exist combined solitary wave solutions in an inhomogeneous fiber system. This is useful in the design of fiber optic amplifiers and in the study of simultaneous propagation of bright and dark solitonlike pulses in femtosecond fiber laser systems or in communication links with distributed dispersion and nonlinearity management. Also, we have discussed the stability of the combined solitary waves under slight violations of the parameter conditions and finite initial perturbations. The results show that the combined waves are still stable under slight violations of the parameter conditions and finite initial perturbations, such as amplitude and white noise. Finally, we have numerically investigated the interaction between two neighboring solitary waves. The results imply that the combined transmission of bright and dark solitary waves can restrict the interaction between neighboring solitary waves to some extent. This is an advantage in improving the information bit rate in ultrahigh-speed optical telecommunication.

This work is supported by the National Natural Science Foundation of China Grants No. 60244006 and No. 60477026, and the Provincial Overseas Scholar Foundation of Shanxi.

[1] G. P. Agrawal, *Nonlinear Fiber Optics* (Academic Press, New York, 1995).
[2] Y. Kodama, J. Stat. Phys. **39**, 597 (1985).
[3] Y. Kodama and A. Hasegawa, IEEE J. Quantum Electron. **23**, 510 (1987).
[4] R. Hirota, J. Math. Phys. **14**, 805 (1973).
[5] N. Sasa and J. Satsuma, J. Phys. Soc. Jpn. **60**, 409 (1991).
[6] M. J. Potasek and M. Tabor, Phys. Lett. A **154**, 449 (1991).
[7] K. Porsezian and K. Nakkeeran, Phys. Rev. Lett. **76**, 3955 (1996).
[8] J. Kim, Q. H. Park, and H. J. Shin, Phys. Rev. E **58**, 6746 (1998).
[9] M. Gedalin, T. C. Scott, and Y. B. Band, Phys. Rev. Lett. **78**, 448 (1997).
[10] S. L. Palacios, A. Guinea, J. M. Fernandez-Diaz, and R. D. Crespo, Phys. Rev. E **60**, R45 (1999).
[11] E. M. Gromov, L. V. Piskunova, and V. V. Tutin, Phys. Lett. A **256**, 153 (1999).
[12] Z. H. Li, L. Li, H. P. Tian, and G. S. Zhou, Phys. Rev. Lett. **84**, 4096 (2000).
[13] W. P. Hong, Opt. Commun. **194**, 217 (2001).
[14] L. Li, Z. H. Li, Z. Y. Xu, G. S. Zhou, and Karl. H. Spatschek, Phys. Rev. E **66**, 046616 (2002).
[15] H. H. Kuehl, J. Opt. Soc. Am. B **5**, 709 (1988).
[16] Y. Kodama, A. Maruta, and A. Hasegawa, Quantum Opt. **6**, 463 (1994).
[17] F. Abdullaeev, *Theory of Solitons in Inhomogeneous Media* (Wiley, New York, 1994).
[18] N. Joshi, Phys. Lett. A **125**, 456 (1987).
[19] P. A. Clarkson, Proc. - R. Soc. Edinburgh, Sect. A: Math. **109**, 109 (1988).
[20] Y.-T. Gao and B. Tian, Comput. Math. Appl. **40**, 1107 (2000).
[21] J. Garnier and F. K. Abdullaev, Physica D **145**, 65 (2000).
[22] J. D. Moores, Opt. Lett. **21**, 555 (1996).
[23] V. N. Serkin and A. Hasegawa, Phys. Rev. Lett. **85**, 4502 (2000); JETP Lett. **72**, 89 (2000); IEEE J. Sel. Top. Quantum Electron. **8**, 418 (2002).
[24] V. N. Serkin and T. L. Belyaeva, JETP Lett. **74**, 573 (2001); Quantum Electron. **31**, 1007 (2001).
[25] H. J. Shin, Phys. Lett. A **294**, 199 (2002).
[26] V. I. Kruglov, A. C. Peacock, and J. D. Harvey, Phys. Rev. Lett. **90**, 113902 (2003).
[27] L. Li, Z. H. Li, S. Q. Li, and G. S. Zhou, Opt. Commun. **234**, 169 (2004).
[28] R. Y. Hao, L. Li, Z. H. Li, and G. S. Zhou, Opt. Commun. **236**, 79 (2004).
[29] E. Papaioannou, D. J. Frantzeskakis, and K. Hizanidis, IEEE J. Quantum Electron. **32**, 145 (1996).
[30] R. Y. Hao, L. Li, Z. H. Li, and G. S. Zhou, Phys. Rev. E **70**, 066603 (2004).
[31] R. C. Yang, R. Y. Hao, L. Li, Z. H. Li, and G. S. Zhou, Opt. Commun. **242**, 285 (2004).